JOURNAL OF COMPUTATIONAL PHYSICS **131,** 299–309 (1997)
ARTICLE NO. CP965596

Numerical Modelling of Wave Propagation in Elastic Rectangular Block Media

Jianwei Zhou and Nader Saffari

Department of Mechanical Engineering, University College London, Torrington Place, London WC1E 7JE, United Kingdom

Received November 20, 1995; revised July 10, 1996

Novel formulations for numerical modelling of elastic waves in block media are developed in this paper. A single differential-difference equation, which can be discretized to give explicit finite difference models of wave propagation in elastic block media, is obtained after incorporating continuity conditions of stresses into the equation of motion. Further decompositions of the differential-difference equation also lead to a parallel algorithm for computing the wave field. © 1997 Academic Press

1. INTRODUCTION

Elastic wave diffraction at multimedia interfaces is an interesting problem encountered in many different applications, including geophysics, seismology, and ultrasonic non-destructive evaluation (NDE). Mathematical models in geophysics and seismology often treat large scale regions of the earth as multi-layered elastic bodies with wavy interfaces between the layers, see Kelly *et al.* [1]. In ultrasonic NDE, small scale defects or inhomogeneities are usually of interest, which include voids, inclusions, and cracks. Reflections, transmissions, and diffractions due to ultrasound interaction with defects in the test material carry crucial information about the properties of the material and provide the basis for ultrasonic NDE, see [2–5].

Any complicated elastic space can be approximated by discrete polygonal elastic sub-spaces (blocks). This might include many problems of practical interest such as elastic wave scattering from regularly shaped inhomogeneities and propagation in stratified media. Curved interfaces can also be approximated as a series of rectilinear steps. A modelling approach which is based on discretization of the computational space into blocks renders itself amenable to numerical solutions using a method such as finite differences, see Harker [6].

The interface between two homogeneous solid half-spaces provides the simplest example of an interface problem in elastic block media. Analytical solutions often exist for such cases, see [7, 8]. The problem of elastic wave propagation in more general block media, however, is much more difficult to solve. There are no complete analytical solutions available. It is therefore necessary to have proper numerical models for understanding the physics of elastic wave propagation and scattering in the more general block media.

There are several approaches for studying elastic block media numerically. The traditional one is to let the wave field in the interior of each individual block be computed from the discretized homogeneous and isotropic elastic wave equation of the block. The wave field along any interface is then computed from the imposition of the continuity of displacements and stresses, see [9] for example. A more general approach treats elastic block media as inhomogeneous media, see Boore [10], Temple [11, 12], and Cunha [13], though special care has to be taken at places where material parameters are discontinuous but stresses have to be continuous. Typically, the discontinuities of the material parameters have to be smoothed over some narrow artificial transition zones. The actual smoothing is usually done by a simple averaging or blending process. Additional computational difficulties may arise from such a treatment. The width of a transition zone is small, normally one or two grid spacings only. Thus material parameters as functions of spatial variables may not be accurately discretized, which can affect the overall accuracy of the numerical model. To overcome this problem, Cunha [13] has tried ''long'' and ''short'' operators on displacements and material parameters separately to minimize the effect of discontinuities in material parameters. In their recent paper, Zahradník and Priolo [14] have used the Dirac delta function and Heaviside's step function to explicitly describe the wave motion and continuity conditions in elastic block media in one single differential equation. This new differential equation is then discretized globally for numerical computations.

In this study, we consider elastic media composed of rectangular blocks also in a global manner. A series of generalized equations of motion will be developed with continuity conditions across interfaces automatically incorporated. We give a detailed derivation and analysis of the generalized equation of motion along horizontal interfaces and list the analogies for vertical and vertex interfaces. Neighbouring blocks do not have to be all distinct. Thus,

0021-9991/97 $25.00

each point in space can be treated as a vertex interface and be associated with a single differential-difference equation that unifies the treatment for interior body nodes, horizontal and vertical interface nodes, and four-media interface vertex nodes in block media. This single differential-difference equation approximates a combination of the equation of motion and the continuity constraint on stresses. The order of approximation can be arbitrarily prescribed. For simplicity, we restrict ourselves to two-dimensional linear time-dependent elasticity and the waves considered in our numerical examples are plane waves. However, much of the mathematics can be extended to three-dimensional situations.

2. INTEGRAL AND DIFFERENTIAL EQUATIONS OF MOTION IN ELASTIC MEDIA

Denote (x, z) as the point of interest in space and $\boldsymbol{u} = \boldsymbol{u}(x, z, t)$ as the displacement vector at the point. For continuity of the displacement field, there should be only one vector value associated with a point in space at any time t. Then the integral form of the equation of motion without body forces is

$$\frac{1}{|\mathbf{V}|}\int_{\mathbf{V}} \rho \boldsymbol{u}_{tt}\, dV = \frac{1}{|\mathbf{V}|}\int_{\partial \mathbf{V}} \boldsymbol{T}_{\hat{\boldsymbol{n}}}\, dS, \tag{1}$$

where for $\mathbf{T}$ being the stress tensor, $\boldsymbol{T}_{\hat{\boldsymbol{n}}} = \mathbf{T}\cdot\hat{\boldsymbol{n}}$ is the stress vector in the direction of the unit outward normal $\hat{\boldsymbol{n}}$ and ρ is the material density. Also in the above equation, $\mathbf{V}$ is an arbitrary volume in space that contains the point (x, z), $\partial\mathbf{V}$ the boundary surface of $\mathbf{V}$ and $|\mathbf{V}|$ the volume of $\mathbf{V}$.

For continuous media, a unique differential form of the equation of motion

$$\rho \boldsymbol{u}_{tt} = \nabla\cdot\mathbf{T} \tag{2}$$

is obtained when $|\mathbf{V}|$ goes to zero. By Hook's law, the stresses can be expressed as

$$\boldsymbol{T}_{\hat{\boldsymbol{x}}} = \begin{bmatrix} T_{xx} \\ T_{xz} \end{bmatrix} = \begin{bmatrix} \lambda+2\mu & 0 \\ 0 & \mu \end{bmatrix}\boldsymbol{u}_x + \begin{bmatrix} 0 & \lambda \\ \mu & 0 \end{bmatrix}\boldsymbol{u}_z \tag{3}$$

and

$$\boldsymbol{T}_{\hat{\boldsymbol{z}}} = \begin{bmatrix} T_{xz} \\ T_{zz} \end{bmatrix} = \begin{bmatrix} 0 & \mu \\ \lambda & 0 \end{bmatrix}\boldsymbol{u}_x + \begin{bmatrix} \mu & 0 \\ 0 & \lambda+2\mu \end{bmatrix}\boldsymbol{u}_z, \tag{4}$$

where $\hat{\boldsymbol{x}}$ and $\hat{\boldsymbol{z}}$ are the unit directional vectors for the x and z axes and λ and μ are the elastic parameters of *isotropic* media. If the media are also *homogeneous* where λ and μ are constants, we have by the definition of the ∇ operator,

$$\begin{aligned}\rho\boldsymbol{u}_{tt} = &\begin{bmatrix} \lambda+2\mu & 0 \\ 0 & \mu \end{bmatrix}\boldsymbol{u}_{xx} + \begin{bmatrix} 0 & \lambda+\mu \\ \lambda+\mu & 0 \end{bmatrix}\boldsymbol{u}_{xz} \\ &+ \begin{bmatrix} \mu & 0 \\ 0 & \lambda+2\mu \end{bmatrix}\boldsymbol{u}_{zz},\end{aligned} \tag{5}$$

as the differential equation of motion.

When (x, z) is situated on an interface of dissimilar materials, there is no longer a unique differential form of the equation of motion corresponding to the integral one. The material density and elastic parameters are now discontinuous. As $|\mathbf{V}|$ goes to zero, the limit of the integral equation (1) will depend on the geometry of $\mathbf{V}$. Moreover, the continuities of displacements and stresses that are automatically satisfied for homogeneous and isotropic media will now have to be further imposed in addition to the equation of motion for general elastic media that support continuous motion.

Consider now the elastic media where the elastic parameters are piecewise constants. Block media are typical examples of such piecewise homogeneous and isotropic elastic media. For an interface point (x, z), the volume $\mathbf{V}$ in (1) that contains (x, z) is a union of several sub-volumes $\mathbf{V}_i$. Within each of these sub-volumes, the density and the elastic parameters are constants. Let us use superscript i for vectors and subscript i for scalars and volumes to indicate values associated with the sub-volume $\mathbf{V}_i$, for example, ρ_i, λ_i, and $\boldsymbol{u}^i_{xz}$. Then the integral equation of motion (1) becomes

$$\sum_{\mathbf{i}} \frac{|\mathbf{V}_i|}{|\mathbf{V}|}\frac{1}{|\mathbf{V}_i|}\int_{\mathbf{V}_i} \rho_i u_{tt}\, dV = \sum_i \frac{|\mathbf{V}_i|}{|\mathbf{V}|}\frac{1}{|\mathbf{V}_i|}\int_{\partial\mathbf{V}_i} \boldsymbol{T}_{\hat{\boldsymbol{n}}}\, dS, \tag{6}$$

since the normal component of the stress tensor $\mathbf{T}$ is continuous across any interface and the unit outward normal vectors paired on the common surface of two adjacent sub-volumes are opposite to each other. Thus by choosing $\mathbf{V}$ such that $|\mathbf{V}_i|/|\mathbf{V}| \to w_i$ as $|\mathbf{V}| \to 0$, we derive from (6)

$$\begin{aligned}\sum_i w_i\rho_i\boldsymbol{u}_{tt} = \sum_i w_i \Bigg\{ &\begin{bmatrix} \lambda_i+2\mu_i & 0 \\ 0 & \mu_i \end{bmatrix}\boldsymbol{u}^i_{xx} \\ &+ \begin{bmatrix} 0 & \lambda_i+\mu_i \\ \lambda_i+\mu_i & 0 \end{bmatrix}\boldsymbol{u}^i_{xz} + \begin{bmatrix} \mu_i & 0 \\ 0 & \lambda_i+2\mu_i \end{bmatrix}\boldsymbol{u}^i_{zz}\Bigg\},\end{aligned} \tag{7}$$

after letting $|\mathbf{V}|$ go to zero. The continuity of displacements is in general satisfied implicitly by the definition of a single $\boldsymbol{u}(x, z, t)$ vector at the point (x, z) for all t. There is thus

no need to use superscript i for $\boldsymbol{u}_{tt}^i$ on the left hand side of (6) and (7).

As a generalization of (5), Eq. (7) is a differential form of the equation of motion at a multimedia interface vertex. It is in fact a weighted average of the elastic wave equations (5) for each medium at that vertex. The weights are not unique as we have commented before. In the next section, we shall demonstrate how these weights can actually be appropriately assigned so that stress-continuity conditions at interface points are incorporated with elastic wave equations to form a class of generalized equation of motion that can be easily implemented in the numerical modelling of wave propagations in elastic block media.

3. GENERALIZED EQUATION OF MOTION FOR INTERFACES IN BLOCK MEDIA

We have in the last section established a differential form of the equation of motion at a multimedia interface vertex. A necessary condition for the development of Eq. (7) is that the component of stress tensor **T** normal to any interface surface is continuous. This necessary condition is also a constraint for continuous motion and hence has to be reflected in any numerical implementations of the equation of motion (7). We limit ourselves to the finite difference implementations in the current study. For this purpose, we shall develop in this section a class of differential-difference equations as generalized equations of motion for interface points.

There are three types of interfaces in rectangular block media. A horizontal interface is described by $z = \text{const}$, a vertical interface is by $x = \text{const}$, and a four-media vertex interface is the intersection of a horizontal interface and a vertical interface with each quarter being occupied by one homogeneous and isotropic medium. It should be noted that the four media do not have to be all distinct.

The discontinuity of the derivatives of $\boldsymbol{u}$ across an interface implies that higher order cross-boundary derivatives are more difficult to discretize and to compute. It then justifies the need for alternative expressions for the second order derivatives in (7). Motivated by the new composed stress-free conditions of Ilan and Loewenthal [18] and by the observation that some of the matrix coefficients in the equation of motion and in the expression of stress vectors are the same, see (3), (4), (5), and (7), we approximate the second order cross-boundary derivatives of $\boldsymbol{u}$ with finite differences and first order derivatives. The first order derivative terms can then be used to combine the stress continuity constraints with the wave equation (7) to form a single differential-difference equation which will be further discretized to give finite difference schemes at interface points.

The following formulae are obtained with successive Taylor expansions

$$\begin{aligned} \boldsymbol{u}_{xx} &= G_l^x[h_x]\boldsymbol{u} - \frac{g_l}{h_x}\boldsymbol{u}_x + O(h_x^l), \\ \boldsymbol{u}_{zz} &= G_l^z[h_z]\boldsymbol{u} - \frac{g_l}{h_z}\boldsymbol{u}_z + O(h_z^l), \end{aligned} \tag{8}$$

with one-sided difference operators $G_l^x[h_x]$ and $G_l^z[h_z]$ defined by

$$G_l^x[h_x]\boldsymbol{u}(x,z,t) = \frac{2}{h_x^2}\sum_{k=0}^{l} a_{l,k}\boldsymbol{u}(x+kh_x, z, t), \tag{9}$$

and

$$G_l^z[h_z]\boldsymbol{u}(x,z,t) = \frac{2}{h_z^2}\sum_{k=0}^{l} a_{l,k}\boldsymbol{u}(x, z+kh_z, t). \tag{10}$$

The coefficients in the above expressions are given by

$$\begin{aligned} g_l &= \sum_{i=1}^{l}\frac{2}{i}, \qquad a_{l,0} = \sum_{k=1}^{l}\binom{l}{k}\frac{(-1)^k}{k^2}, \\ a_{l,k} &= \binom{l}{k}\frac{(-1)^{k+1}}{k^2}, \qquad k = 1, ..., l. \end{aligned} \tag{11}$$

We begin by examining the derivation of the new composed *stress-free* boundary condition of Ilan and Loewenthal [18]. Let $z = (z_0)_+$ be a stress-free surface that bounds the solid occupying $z \geq z_0$. Instead of using

$$\begin{bmatrix} 0 & \mu \\ \lambda & 0 \end{bmatrix}\boldsymbol{u}_x + \begin{bmatrix} \mu & 0 \\ 0 & \lambda+2\mu \end{bmatrix}\boldsymbol{u}_z = \boldsymbol{0}$$

to describe the stress-free boundary, see (4), Ilan and Loewenthal constructed a boundary condition based on a composition of the above equation and the elastic wave equation (5). By writing

$$\boldsymbol{u}(x, z_0 + h_z, t) = \boldsymbol{u} + h_z\boldsymbol{u}_z + (h_z^2/2)\boldsymbol{u}_{zz},$$

they derived

$$\begin{bmatrix} \mu & 0 \\ 0 & \lambda+2\mu \end{bmatrix}\boldsymbol{u}_{zz} = \begin{bmatrix} \mu & 0 \\ 0 & \lambda+2\mu \end{bmatrix} G_1^z[h]\boldsymbol{u} + \frac{2}{h}\begin{bmatrix} 0 & \mu \\ \lambda & 0 \end{bmatrix}\boldsymbol{u}_x$$

where from Eqs. (8), (10), and (11),

$$G_1^z[h]\,\boldsymbol{u}(x, z_0, t) = \frac{2}{h^2}\left(\boldsymbol{u}(x, z_0+h, t) - \boldsymbol{u}(z, z_0, t)\right).$$

This expression for $\boldsymbol{u}_{zz}$ was then used to replace the $\boldsymbol{u}_{zz}$ term in the wave equation (5) to produce the new composed stress-free condition

$$\rho \boldsymbol{u}_{tt} = \begin{bmatrix} \lambda + 2\mu & 0 \\ 0 & \mu \end{bmatrix} \boldsymbol{u}_{xx} + \begin{bmatrix} 0 & \lambda + \mu \\ \lambda + \mu & 0 \end{bmatrix} \boldsymbol{u}_{xz} + \begin{bmatrix} \mu & 0 \\ 0 & \lambda + 2\mu \end{bmatrix} G_1^z[h]\boldsymbol{u} + \frac{2}{h} \begin{bmatrix} 0 & \mu \\ \lambda & 0 \end{bmatrix} \boldsymbol{u}_x. \tag{12}$$

In order to avoid tediousness, we only describe the development of the generalized equation of motion for a horizontal interface in detail. A simple analogy will be applied for a vertical interface. Outlines of the development of the generalized equation of motion for a vertex interface will be summarized with the list of final equations.

Suppose that (x, z) is lying on the horizontal interface between medium 1 and medium 2 that are described by $z' \geq z$ and $z' \leq z$, respectively. Then the equation of motion (7) in this particular case becomes

$$\begin{aligned} \mathbf{0} = L\boldsymbol{u} = -\boldsymbol{u}_{tt} \\ + \frac{w_1}{w_1\rho_1 + w_2\rho_2} \left\{ \begin{bmatrix} \lambda_1 + 2\mu_1 & 0 \\ 0 & \mu_1 \end{bmatrix} \boldsymbol{u}_{xx}^1 + \begin{bmatrix} 0 & \lambda_1 + \mu_1 \\ \lambda_1 + \mu_1 & 0 \end{bmatrix} \boldsymbol{u}_{xz}^1 \right. \\ \left. + \begin{bmatrix} \mu_1 & 0 \\ 0 & \lambda_1 + 2\mu_1 \end{bmatrix} \boldsymbol{u}_{zz}^1 \right\} + \frac{w_2}{w_1\rho_1 + w_2\rho_2} \left\{ \begin{bmatrix} \lambda_2 + 2\mu_2 & 0 \\ 0 & \mu_2 \end{bmatrix} \boldsymbol{u}_{xx}^2 \right. \\ \left. + \begin{bmatrix} 0 & \lambda_2 + \mu_2 \\ \lambda_2 + \mu_2 & 0 \end{bmatrix} \boldsymbol{u}_{xz}^2 + \begin{bmatrix} \mu_2 & 0 \\ 0 & \lambda_2 + 2\mu_2 \end{bmatrix} \boldsymbol{u}_{zz}^2 \right\}. \end{aligned} \tag{13}$$

Denote the vertical grid spacings for finite differences as h_{z1} in medium 1 and h_{z2} in medium 2 with $\boldsymbol{h} = (h_{z1}, h_{z2})$. We may then let $w_1/h_{z1} = w_2/h_{z2}$, which can be achieved, for example, by choosing

$$\mathbf{V}_1 = \mathbf{V}_1(r) = [x - ra, x + ra] \times [z, z + rh_{z1}]$$

and

$$\mathbf{V}_2 = \mathbf{V}_2(r) = [x - ra, x + ra] \times [z - rh_{z2}, z]$$

for $r \to 0$. Here $a > 0$ is arbitrary and the interface is aligned to a grid line. We also use (4) to rewrite (8) as

$$\begin{bmatrix} \mu_1 & 0 \\ 0 & \lambda_1 + 2\mu_1 \end{bmatrix} \boldsymbol{u}_{zz}^1 = \begin{bmatrix} \mu_1 & 0 \\ 0 & \lambda_1 + 2\mu_1 \end{bmatrix} G_l^z[h_{z1}]\boldsymbol{u} + \frac{g_l}{h_{z1}} \begin{bmatrix} 0 & \mu_1 \\ \lambda_1 & 0 \end{bmatrix} \boldsymbol{u}_x - \frac{g_l}{h_{z1}} \boldsymbol{T}_{\hat{\boldsymbol{z}}}^1 + O(h_{z1}^l) \tag{14}$$

and

$$\begin{bmatrix} \mu_2 & 0 \\ 0 & \lambda_2 + 2\mu_2 \end{bmatrix} \boldsymbol{u}_{zz}^2 = \begin{bmatrix} \mu_2 & 0 \\ 0 & \lambda_2 + 2\mu_2 \end{bmatrix} G_l^z[-h_{z2}]\boldsymbol{u} - \frac{g_l}{h_{z2}} \begin{bmatrix} 0 & \mu_2 \\ \lambda_2 & 0 \end{bmatrix} \boldsymbol{u}_x + \frac{g_l}{h_{z2}} \boldsymbol{T}_{\hat{\boldsymbol{z}}}^2 + O(h_{z2}^l). \tag{15}$$

The generalized equation of motion for a horizontal interface is then derived by substituting the above two equations into (13),

$$\begin{aligned} \mathbf{0} = L_h\boldsymbol{u} = -\boldsymbol{u}_{tt} \\ + \gamma_1 \left\{ \begin{bmatrix} \lambda_1 + 2\mu_1 & 0 \\ 0 & \mu_1 \end{bmatrix} \boldsymbol{u}_{xx} + \begin{bmatrix} 0 & \lambda_1 + \mu_1 \\ \lambda_1 + \mu_1 & 0 \end{bmatrix} \boldsymbol{u}_{xz}^1 \right. \\ \left. + \begin{bmatrix} \mu_1 & 0 \\ 0 & \lambda_1 + 2\mu_1 \end{bmatrix} G_l^z[h_{z1}]\boldsymbol{u} + \frac{g_l}{h_{z_1}} \begin{bmatrix} 0 & \mu_1 \\ \lambda_1 & 0 \end{bmatrix} \boldsymbol{u}_x \right\} \\ + \gamma_2 \left\{ \begin{bmatrix} \lambda_2 + 2\mu_2 & 0 \\ 0 & \mu_2 \end{bmatrix} \boldsymbol{u}_{xx} + \begin{bmatrix} 0 & \lambda_2 + \mu_2 \\ \lambda_2 + \mu_2 & 0 \end{bmatrix} \boldsymbol{u}_{xz}^2 \right. \\ \left. + \begin{bmatrix} \mu_2 & 0 \\ 0 & \lambda_2 + 2\mu_2 \end{bmatrix} G_l^z[-h_{z2}]\boldsymbol{u} - \frac{g_l}{h_{z2}} \begin{bmatrix} 0 & \mu_2 \\ \lambda_2 & 0 \end{bmatrix} \boldsymbol{u}_x \right\}, \end{aligned} \tag{16}$$

where we assumed $\boldsymbol{T}_{\hat{\boldsymbol{z}}}^1 = \boldsymbol{T}_{\hat{\boldsymbol{z}}}^2$ and

$$\gamma_1 = \frac{h_{z1}}{h_{z1}\rho_1 + h_{z2}\rho_2}, \qquad \gamma_2 = \frac{h_{z2}}{h_{z1}\rho_1 + h_{z2}\rho_2}. \tag{17}$$

Note that we have dropped superscripts on $\boldsymbol{u}$, $\boldsymbol{u}_x$, and $\boldsymbol{u}_{xx}$ terms because of the continuity of displacements. The error term omitted in (16) is $O(h_{z1}^l + h_{z2}^l)$ or $O(\boldsymbol{h}^l)$ for short. In practice, the order of approximation l from differential-difference equation (16) to the differential equation of motion (13) is chosen as either 1 or 2 with continuous stresses.

We now discuss the conditional consistency of (16) with the original stress-continuity condition

$$\boldsymbol{T}_{\hat{\boldsymbol{z}}}^1(x, z, t) = \boldsymbol{T}_{\hat{\boldsymbol{z}}}^2(x, z, t) \tag{18}$$

and with wave equation (13). Let $\boldsymbol{u}^{\boldsymbol{h}}$ be the approximate displacement field that satisfies (16), that is, $L_h\boldsymbol{u}^{\boldsymbol{h}} = \mathbf{0}$, and denote $\boldsymbol{T}_{\hat{\boldsymbol{z}}}^{1,\boldsymbol{h}}$ and $\boldsymbol{T}_{\hat{\boldsymbol{z}}}^{2,\boldsymbol{h}}$ as the approximate stresses normal to the horizontal interface that are computed in medium 1

and medium 2, respectively. A simple algebraic process then leads to

$$\begin{aligned} -L\boldsymbol{u}^{\boldsymbol{h}} &= L_h\boldsymbol{u}^{\boldsymbol{h}} - L\boldsymbol{u}^{\boldsymbol{h}} \\ &= \frac{g_l}{h_{z1}\rho_1 + h_{z2}\rho_2}(\boldsymbol{T}_{\hat{\boldsymbol{z}}}^{1,\boldsymbol{h}} - \boldsymbol{T}_{\hat{\boldsymbol{z}}}^{2,\boldsymbol{h}}) + O(\boldsymbol{h}^l). \end{aligned} \tag{19}$$

Thus if we assume that $\boldsymbol{u}^{\boldsymbol{h}}$ has uniformly bounded second derivatives for $\boldsymbol{h} \to \boldsymbol{0}$, then

$$\lim_{\boldsymbol{h}\to\boldsymbol{0}}(\boldsymbol{T}_{\hat{\boldsymbol{z}}}^{1,\boldsymbol{h}} - \boldsymbol{T}_{\hat{\boldsymbol{z}}}^{2,\boldsymbol{h}}) = \boldsymbol{0}, \tag{20}$$

which implies the consistency with the original stress continuity condition (18). Further assuming $\boldsymbol{T}_{\hat{\boldsymbol{z}}}^{1,\boldsymbol{h}} - \boldsymbol{T}_{\hat{\boldsymbol{z}}}^{2,\boldsymbol{h}} \to \boldsymbol{0}$ at a faster rate such that

$$\boldsymbol{T}_{\hat{\boldsymbol{z}}}^{1,\boldsymbol{h}} - \boldsymbol{T}_{\hat{\boldsymbol{z}}}^{2,\boldsymbol{h}} = o(\boldsymbol{h}), \tag{21}$$

then we have

$$\lim_{\boldsymbol{h}\to\boldsymbol{0}} L\,\boldsymbol{u}^{\boldsymbol{h}} = \boldsymbol{0}, \tag{22}$$

which implies the consistency with wave equation (13).

The above discussion shows that our generalized equation of motion (16) is a neat combination of the wave equation and the constraints of stresses at interface points for continuous elastic media. Stress-continuity constraints are more dominant in (16) since (20) holds under mild assumptions. For finite difference modelling, Eq. (16) should mix well with the wave equation (5) in the two homogeneous and isotropic media that form the horizontal interface in the sense that (16) reduces to an approximation of (5) with $\boldsymbol{u}_{zz}$ replaced by a finite difference if the two media are the same.

Before moving on to other types of interfaces, we point out that stress-free conditions are actually included in (16) although the analysis is for stress-continuity conditions. If one of the two adjacent media, medium 2 say, is vacuum, then $\rho_2 = 0$, $\lambda_2 = 0$, and $\mu_2 = 0$. Equation (16) degenerates to

$$\begin{aligned} \boldsymbol{u}_{tt} = &\begin{bmatrix} \alpha_1^2 & 0 \\ 0 & \beta_1^2 \end{bmatrix}\boldsymbol{u}_{xx} + \begin{bmatrix} 0 & \alpha_1^2 - \beta_1^2 \\ \alpha_1^2 - \beta_1^2 & 0 \end{bmatrix}\boldsymbol{u}_{xz} \\ &+ \begin{bmatrix} \beta_1^2 & 0 \\ 0 & \alpha_1^2 \end{bmatrix} G_l^z[h_{z1}]\boldsymbol{u} + \frac{g_l}{h_{z1}}\begin{bmatrix} 0 & \beta_1^2 \\ \alpha_1^2 - 2\beta_1^2 & 0 \end{bmatrix}\boldsymbol{u}_x, \end{aligned} \tag{23}$$

which becomes the new composed stress-free condition due to Ilan and Loewenthal [18] for $l = 1$, see (12). Here we have used $\lambda_1 = \rho_1(\alpha_1^2 - 2\beta_1^2)$ and $\mu_1 = \rho_1\beta_1^2$.

Let us now consider a vertical interface point. Suppose that (x, z) is lying on the interface between medium 1 and medium 2 that are described by $x' \geq x$ and $x' \leq x$, respectively. As an analogy to the case of a horizontal interface, we immediately derive the following generalized equation of motion for a vertical interface

$$\begin{aligned} \boldsymbol{u}_{tt} = &\gamma_1\left\{\begin{bmatrix} \lambda_1 + 2\mu_1 & 0 \\ 0 & \mu_1 \end{bmatrix} G_l^x[h_{x1}]\boldsymbol{u} + \frac{g_l}{h_{x1}}\begin{bmatrix} 0 & \lambda_1 \\ \mu_1 & 0 \end{bmatrix}\boldsymbol{u}_z \right. \\ &\left. + \begin{bmatrix} 0 & \lambda_1 + \mu_1 \\ \lambda_1 + \mu_1 & 0 \end{bmatrix}\boldsymbol{u}_{xz}^1 + \begin{bmatrix} \mu_1 & 0 \\ 0 & \lambda_1 + 2\mu_1 \end{bmatrix}\boldsymbol{u}_{zz}\right\} \\ &+ \gamma_2\left\{\begin{bmatrix} \lambda_2 + 2\mu_2 & 0 \\ 0 & \mu_2 \end{bmatrix} G_l^x[-h_{x2}]\boldsymbol{u} - \frac{g_l}{h_{x2}}\begin{bmatrix} 0 & \lambda_2 \\ \mu_2 & 0 \end{bmatrix}\boldsymbol{u}_z \right. \\ &\left. + \begin{bmatrix} 0 & \lambda_2 + \mu_2 \\ \lambda_2 + \mu_2 & 0 \end{bmatrix}\boldsymbol{u}_{xz}^2 + \begin{bmatrix} \mu_2 & 0 \\ 0 & \lambda_2 + 2\mu_2 \end{bmatrix}\boldsymbol{u}_{zz}\right\} \end{aligned} \tag{24}$$

by substituting

$$\begin{aligned} \begin{bmatrix} \lambda_1 + 2\mu_1 & 0 \\ 0 & \mu_1 \end{bmatrix}\boldsymbol{u}_{xx}^1 = &\begin{bmatrix} \lambda_1 + 2\mu_1 & 0 \\ 0 & \mu_1 \end{bmatrix} G_l^x[h_{x1}]\boldsymbol{u} \\ &+ \frac{g_l}{h_{x1}}\begin{bmatrix} 0 & \lambda_1 \\ \mu_1 & 0 \end{bmatrix}\boldsymbol{u}_z - \frac{g_l}{h_{x1}}\boldsymbol{T}_{\hat{\boldsymbol{x}}}^1 + O(h_1^l) \end{aligned} \tag{25}$$

and

$$\begin{aligned} \begin{bmatrix} \lambda_2 + 2\mu_2 & 0 \\ 0 & \mu_2 \end{bmatrix}\boldsymbol{u}_{zz}^2 = &\begin{bmatrix} \lambda_2 + 2\mu_2 & 0 \\ 0 & \mu_2 \end{bmatrix} G_l^x[-h_{x2}]\,\boldsymbol{u} \\ &- \frac{g_l}{h_{x2}}\begin{bmatrix} 0 & \lambda_2 \\ \mu_2 & 0 \end{bmatrix}\boldsymbol{u}_z + \frac{g_l}{h_{x2}}\boldsymbol{T}_{\hat{\boldsymbol{x}}}^2 + O(h_2^l) \end{aligned} \tag{26}$$

into (7). The coefficients γ_1 and γ_2 in (24) are given by (17), but with h_{z1} and h_{z2} replaced by h_{x1} and h_{x2}, respectively.

Finally, we examine the situation of a four-media vertex interface. Let (x, z) be such a vertex and the first of the four homogeneous and isotropic media be bounded by $x' \geq x$ and $z' \geq z$, the second by $x' \geq x$ and $z' \leq z$, the third by $x' \leq x$ and $z' \leq z$, and the fourth by $x' \leq x$ and $z' \geq z$. We also assume that the grid spacings for finite differences are $h_1 = h_{z1}$ for $z' > z$, $h_2 = h_{x1}$ for $x' > x$, $h_3 = h_{z2}$ for $z' < z$, and $h_4 = h_{x2}$ for $x' < x$.

We choose $w_i = h_i h_{i+1}/(h_1 + h_3)\,(h_2 + h_4)$, for $1 \le i \le 4$, with h_5 interpreted as h_1. It can be achieved by letting

$$\begin{aligned}
\mathbf{V}_1 &= \mathbf{V}_1(r) = [x, x + rh_{x1}] \times [z, z + rh_{z1}] \\
&= [x, x + rh_2] \times [z, z + rh_1], \\
\mathbf{V}_2 &= \mathbf{V}_2(r) = [x, x + rh_{x1}] \times [z - rh_{z2}, z] \\
&= [x, x + rh_2] \times [z - rh_3, z], \\
\mathbf{V}_3 &= \mathbf{V}_3(r) = [x - rh_{x2}, x] \times [z - rh_{z2}, z] \\
&= [x - rh_4, x] \times [z - rh_3, z],
\end{aligned}$$

and

$$\begin{aligned}
\mathbf{V}_4 &= \mathbf{V}_4(r) = [x - rh_{x2}, x] \times [z, z + rh_{z1}] \\
&= [x - rh_4, x] \times [z, z + rh_1],
\end{aligned}$$

for $r \to 0$. The equation of motion (7) in this case becomes

$$\begin{aligned}
\boldsymbol{u}_{tt} = \gamma_1 \Bigg\{ & \begin{bmatrix} \lambda_1 + 2\mu_1 & 0 \\ 0 & \mu_1 \end{bmatrix} \boldsymbol{u}^1_{xx} + \begin{bmatrix} 0 & \lambda_1 + \mu_1 \\ \lambda_1 + \mu_1 & 0 \end{bmatrix} \boldsymbol{u}^1_{xz} \\
& + \begin{bmatrix} \mu_1 & 0 \\ 0 & \lambda_1 + 2\mu_1 \end{bmatrix} \boldsymbol{u}^1_{zz} \Bigg\} + \gamma_2 \Bigg\{ \begin{bmatrix} \lambda_2 + 2\mu_2 & 0 \\ 0 & \mu_2 \end{bmatrix} \boldsymbol{u}^2_{xx} \\
& + \begin{bmatrix} 0 & \lambda_2 + \mu_2 \\ \lambda_2 + \mu_2 & 0 \end{bmatrix} \boldsymbol{u}^2_{xz} + \begin{bmatrix} \mu_2 & 0 \\ 0 & \lambda_2 + 2\mu_2 \end{bmatrix} \boldsymbol{u}^2_{zz} \Bigg\} \\
& + \gamma_3 \Bigg\{ \begin{bmatrix} \lambda_3 + 2\mu_3 & 0 \\ 0 & \mu_3 \end{bmatrix} \boldsymbol{u}^3_{xx} + \begin{bmatrix} 0 & \lambda_3 + \mu_3 \\ \lambda_3 + \mu_3 & 0 \end{bmatrix} \boldsymbol{u}^3_{xz} \\
& + \begin{bmatrix} \mu_3 & 0 \\ 0 & \lambda_3 + 2\mu_3 \end{bmatrix} \boldsymbol{u}^3_{zz} \Bigg\} + \gamma_4 \Bigg\{ \begin{bmatrix} \lambda_4 + 2\mu_4 & 0 \\ 0 & \lambda_4 \end{bmatrix} \boldsymbol{u}^4_{xx} \\
& + \begin{bmatrix} 0 & \lambda_4 + \mu_4 \\ \lambda_4 + \mu_4 & 0 \end{bmatrix} \boldsymbol{u}^4_{xz} + \begin{bmatrix} \mu_4 & 0 \\ 0 & \lambda_4 + 2\mu_4 \end{bmatrix} \boldsymbol{u}^4_{zz} \Bigg\},
\end{aligned} \tag{27}$$

where

$$\gamma_i = \frac{h_i h_{i+1}}{h_1 h_2 \rho_1 + h_2 h_3 \rho_2 + h_3 h_4 \rho_3 + h_4 h_1 \rho_4}, \qquad i = 1, 2, 3, 4. \tag{28}$$

Second order cross-boundary derivatives $\boldsymbol{u}_{xx}$ and $\boldsymbol{u}_{zz}$ in (27) can be approximated as before by a combination of lower order terms. The choice of $w_i = h_i h_{i+1}/(h_1 + h_3)\,(h_2 + h_4)$, enables us to incorporate stress-continuity constraints into (27) through the approximation. After replacing all second order cross-boundary derivatives with lower order term approximations, we derive the generalized equation of motion for a vertex interface

$$\begin{aligned}
\boldsymbol{u}_{tt} = \gamma_1 \Bigg\{ & \begin{bmatrix} \lambda_1 + 2\mu_1 & 0 \\ 0 & \mu_1 \end{bmatrix} G^x_l[h_{x1}]\mathbf{u}^1 + \frac{g_l}{h_{x1}} \begin{bmatrix} 0 & \lambda_1 \\ \mu_1 & 0 \end{bmatrix} \boldsymbol{u}^1_z \\
& + \begin{bmatrix} \mu_1 & 0 \\ 0 & \lambda_1 + 2\mu_1 \end{bmatrix} G^z_l[h_{z1}]\boldsymbol{u}^1 + \frac{g_l}{h_{z1}} \begin{bmatrix} 0 & \mu_1 \\ \lambda_1 & 0 \end{bmatrix} \boldsymbol{u}^1_x \Bigg\} \\
& + \gamma_2 \Bigg\{ \begin{bmatrix} \lambda_2 + 2\mu_2 & 0 \\ 0 & \mu_2 \end{bmatrix} G^x_l[h_{x1}]\boldsymbol{u}^2 + \frac{g_l}{h_{x1}} \begin{bmatrix} 0 & \lambda_2 \\ \mu_2 & 0 \end{bmatrix} \boldsymbol{u}^2_z \\
& + \begin{bmatrix} \mu_2 & 0 \\ 0 & \lambda_2 + 2\mu_2 \end{bmatrix} G^z_l[-h_{z2}]\boldsymbol{u}^2 - \frac{g_l}{h_{z2}} \begin{bmatrix} 0 & \mu_2 \\ \lambda_2 & 0 \end{bmatrix} \boldsymbol{u}^2_x \Bigg\} \\
& + \gamma_3 \Bigg\{ \begin{bmatrix} \lambda_3 + 2\mu_3 & 0 \\ 0 & \mu_3 \end{bmatrix} G^x_l[-h_{x2}]\boldsymbol{u}^3 - \frac{g_l}{h_{x2}} \begin{bmatrix} 0 & \lambda_3 \\ \mu_3 & 0 \end{bmatrix} \boldsymbol{u}^3_z \\
& + \begin{bmatrix} \mu_3 & 0 \\ 0 & \lambda_3 + 2\mu_3 \end{bmatrix} G^z_l[-h_{z2}]\boldsymbol{u}^3 - \frac{g_l}{h_{z2}} \begin{bmatrix} 0 & \mu_3 \\ \lambda_3 & 0 \end{bmatrix} \boldsymbol{u}^3_x \Bigg\} \\
& + \gamma_4 \Bigg\{ \begin{bmatrix} \lambda_4 + 2\mu_4 & 0 \\ 0 & \mu_4 \end{bmatrix} G^x_l[-h_{x2}]\boldsymbol{u}^4 - \frac{g_l}{h_{x2}} \begin{bmatrix} 0 & \lambda_4 \\ \mu_4 & 0 \end{bmatrix} \boldsymbol{u}^4_z \\
& + \begin{bmatrix} \mu_4 & 0 \\ 0 & \lambda_4 + 2\mu_4 \end{bmatrix} G^z_l[h_{z1}]\boldsymbol{u}^4 + \frac{g_l}{h_{z1}} \begin{bmatrix} 0 & \mu_4 \\ \lambda_4 & 0 \end{bmatrix} \boldsymbol{u}^4_x \Bigg\} \\
& + \sum_{i=1}^{4} \gamma_i \begin{bmatrix} 0 & \lambda_i + \mu_i \\ \lambda_i + \mu_i & 0 \end{bmatrix} \boldsymbol{u}^i_{xz}.
\end{aligned} \tag{29}$$

The four media meeting at the vertex (x, z) do not have to be all different. Various combinations of blocks with similar and dissimilar materials lead to many interesting interface situations. We list some common ones here. If all four blocks associated with (x, z) are of the same material, (29) reduces to (5) with second order derivatives $\boldsymbol{u}_{xx}$ and $\boldsymbol{u}_{zz}$ discretized as finite differences. If the four blocks are paired so that medium 1 and medium 4 are the same and so are medium 2 and medium 3, then (29) reduces to (16) with $\boldsymbol{u}_{xx}$ discretized. With one/three of the four media becoming vacuum, we obtain conditions for 270°/90° stress-free corners that Alterman and Loewenthal [9] had studied. In fact for finite-difference modelling, we may use (29) as a unified governing equation for elastic waves in block media.

It is possible to extend our approach further and thus allow more degrees of freedom in the final differential-difference formulation. For example, we may use

$$\begin{bmatrix}\mu_1 & 0\\ 0 & \lambda_1+2\mu_1\end{bmatrix}\boldsymbol{u}^1_{zz}=\sigma\begin{bmatrix}\mu_1 & 0\\ 0 & \lambda_1+2\mu_1\end{bmatrix}G^z_l[h_1]\boldsymbol{u}^1$$
$$+\sigma(\delta-1)\frac{g_l}{h_1}\begin{bmatrix}\mu_1 & 0\\ 0 & \lambda_1+2\mu_1\end{bmatrix}\boldsymbol{u}^1_z \qquad (30)$$
$$+\sigma\delta\frac{g_l}{h_1}\begin{bmatrix}0 & \mu_1\\ \lambda_1 & 0\end{bmatrix}\boldsymbol{u}^1_x+(1-\sigma)\begin{bmatrix}\mu_1 & 0\\ 0 & \lambda_1+2\mu_1\end{bmatrix}\boldsymbol{u}^1_{zz}$$
$$-\sigma\delta\frac{g_l}{h_1}\boldsymbol{T}^1_{\tilde{z}}+O(h_1^l)$$

instead of (14) and similar alternative expressions to manipulate second order cross-boundary derivative terms. The parameters σ and δ are useful for balancing the dominance of wave equations and stress constraints in the final formulation. They may also be adjusted to improve the stability of finite difference schemes that are constructed from the differential-difference formulation.

4. NUMERICAL IMPLEMENTATION AND EXAMPLES

For finite difference modelling, equations like (29) have to be further discretized. All derivative terms should be approximated by finite differences to appropriate orders of accuracy in accordance with the value of l that has been specified for differential-difference equations (16), (24), and (29). We fix $l = 2$ because second order methods are sufficient for our applications. Higher order schemes can be achieved for larger l.

Formulas of finite difference approximations used to develop our second order finite difference model are

$$f'(x)=\frac{1}{12h}\{8f(x+h)-8f(x-h)-f(x+2h)$$
$$+f(x-2h)\}+O(h^4)=\frac{1}{6h}\{-11f(x)$$
$$+18f(x+h)-9f(x+2h)+2f(x+3h)\}$$
$$+O(h^3)=\frac{1}{6h}\{-2f(x-h)-3f(x)+6f(x+h)$$
$$-f(x+2h)\}+O(h^3), \qquad (31)$$
$$f''(x)=\frac{1}{h^2}\{f(x+h)-2f(x)+f(x-h)\}+O(h^2)$$
$$=\frac{1}{h^2}\{2f(x)-5f(x+h)+4f(x+2h)$$
$$-f(x+3h)\}+O(h^2), \qquad (32)$$

and

$$F_{xz}(x,z)=\frac{1}{4h_xh_z}\{4F(x+h_x,z+h_z)-4F(x-h_x,z+h_z)$$
$$-F(x+h_x,z+2h_z)+F(x-h_x,z+2h_z)$$
$$-3F(x+h_x,z)+3F(x-h_x,z)]\}+O(h_x^2+h_z^2)$$
$$=\frac{1}{2h_xh_z}\{-5F(x+h_x,z)-5F(x,z+h_z) \qquad (33)$$
$$-F(x+2h_x,z+h_z)-F(x+h_x,z+2h_z)$$
$$+4F(x,z)+F(x+2h_x,z)+6F(x+h_x,z+h_z)$$
$$+F(x,z+2h_z)\}+O(h_x^2+h_z^2).$$

Each of the derivative terms in the unified governing equation for elastic waves (29) can now be approximated in a conventional manner by a finite difference by using the above expressions with the overall accuracy being second order. For example, one may substitute $\boldsymbol{u}^2_{zz}(x,\ z,\ t) = \boldsymbol{u}_{zz}(x+,\ z-,\ t)$ with any of the right hand sides of (32) by regarding z as the variable x in (32) and by letting $h = -h_{z2}$. Denote $\boldsymbol{u}_{i,j,k} = \boldsymbol{u}(x_0 + ih_x,\ z_0 + jh_z,\ t_0 + kh_t)$. We obtain from (29),

$$\boldsymbol{u}_{i,j,k+1}=2\boldsymbol{u}_{i,j,k}-\boldsymbol{u}_{i,j,k-1}+h_t^2P_{i,j,k}(\boldsymbol{u}) \qquad (34)$$

for calculating the wave field by forward iterations in time with $P_{i,j,k}(\boldsymbol{u})$ representing the finite difference approximation of the right hand side of (29) at the point referenced as $(x_0 + ih_x,\ z_0 + jh_z)$ for time level k.

The grid spacings in our finite difference formulation are also required to satisfy

$$h_t\le\min\left\{\frac{h_xh_z}{\sqrt{\alpha^2h_x^2+\beta^2h_z^2}},\frac{h_xh_z}{\sqrt{\alpha^2h_z^2+\beta^2h_x^2}}\right\}, \qquad (35)$$

where α and β are the compressional and shear velocities of the media, following the stability analysis of Alterman and Loewenthal [9] on an infinite homogeneous domain.

Along the sides of the rectangular computational domain, particular second order absorbing boundary conditions of Zhou and Saffari [15] are deployed. As shown in [15], these absorbing boundary conditions work for a wide range of incidences for both compressional and shear incident waves. Although an often negligibly small distortion may result in the numerical solution, the introduction of artificial absorbing boundaries enables us to choose smaller computational domains sufficiently covering the area of interest, for more efficient and speedy numerical solutions.

We wish to show three examples here. The first has a half space of gold perfectly bonded on top of a half space

of aluminium. A compressional vertical pulse wave travels upwards from the lower half space of aluminium across the interface to the upper half space of gold. An analytical solution is given by

$$\boldsymbol{u}(x, z, t) = \begin{cases} \phi(z + \alpha_a t)\boldsymbol{q}(1) + R\phi(-z + \alpha_a t)\boldsymbol{q}(-1), & z \geq 0 \\ T\phi((\alpha_a/\alpha_g)z + \alpha_a t)\boldsymbol{q}(\alpha_a/\alpha_g), & z \leq 0 \end{cases} \tag{36}$$

in terms of a potential function ϕ where

$$\boldsymbol{q}(\eta) = \begin{bmatrix} 0 \\ \eta \end{bmatrix}, \qquad R = \frac{\alpha_g\rho_g - \alpha_a\rho_a}{\alpha_g\rho_g + \alpha_a\rho_a}, \qquad T = \frac{2\alpha_g\rho_a}{\alpha_g\rho_g + \alpha_a\rho_a}. \tag{37}$$

Here, subscripts a and g are used to indicate material parameters of aluminium and gold, respectively. Thus, $\alpha_a = 6398$ m/sec, $\beta_a = 3122$ m/sec, $\rho_a = 2700$ Kg/m^3, and $\alpha_g = 3240$ m/sec, $\beta_g = 1200$ m/sec, $\rho_g = 19300$ Kg/m^3. The computational domain is uniformly discretized with the interface aligned with the central horizontal grid line. The grid spacings are set to

$$h_x = h_z = \frac{\alpha_a}{48f}, \qquad h_t = 0.9\frac{h_x}{\sqrt{\alpha_a^2 + \beta_a^2}}$$

with an operating frequency of $f = 1$ MHz assumed, which implies that there are about 20 nodes per wavelength. We also let the potential function $\phi(\xi)$ be taken as the smooth δ-shaped function

$$\langle\delta(\xi)\rangle = \frac{(\xi+5\Delta)_+^4 - 5(\xi+3\Delta)_+^4 + 10(\xi+\Delta)_+^4 - 10(\xi-\Delta)_+^4 + 5(\xi-3\Delta)_+^4 - (\xi-5\Delta)_+^4}{5520\Delta}$$

with $\Delta = 7h_x$, see Ilan *et al.* [16]. We compute the numerical results of the displacement field with the horizontal interface implemented as either a first order or a second order scheme of the generalized equation of motion (16). The first order scheme is essentially the new composed condition of [17, 18]. The computational domain consists of 240 grids horizontally and 160 grids vertically. For testing the stability of these finite difference schemes of the generalized equation of motion for a horizontal interface, we impose periodic boundary conditions on the two vertical boundaries of the computational domain. The vertical components of displacement at points, fifty grid spacings away from the interface on either side, are recorded for five hundred time levels. The numerical results are then compared with the analytical solution. Both sets of numerical results are found to be in excellent agreement with the analytical solution, see Figs. 1 and 2. Magnitudes of errors are small for both first and second order implementations due to the simplicity of the problem. Overall, the l_2-norm of errors of the second order scheme over the five hundred time levels is 9% smaller than that of the first order scheme.

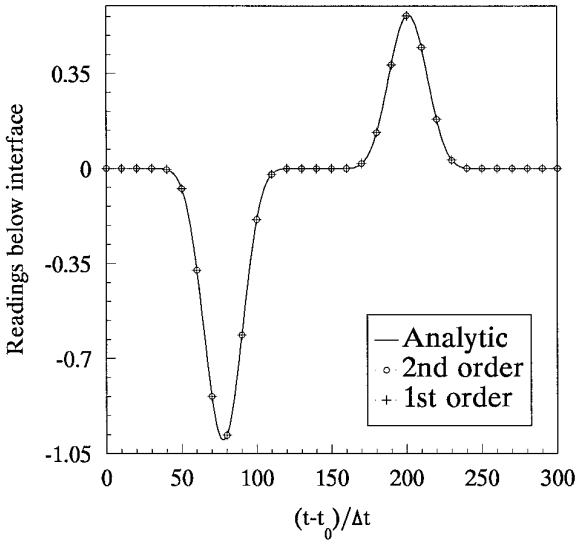

FIG. 1. Magnitude of the incident pulse and the reflection.

The second example is about a particular inverse material inclusion. We examine two perfectly bonded small blocks (aluminium on top of gold) embedded along the interface of two otherwise perfectly bonded half-spaces of solids (gold on top of aluminium), see Fig. 3. These two materials have been chosen because they provide a large acoustic mismatch as well as two very different β/α ratios.

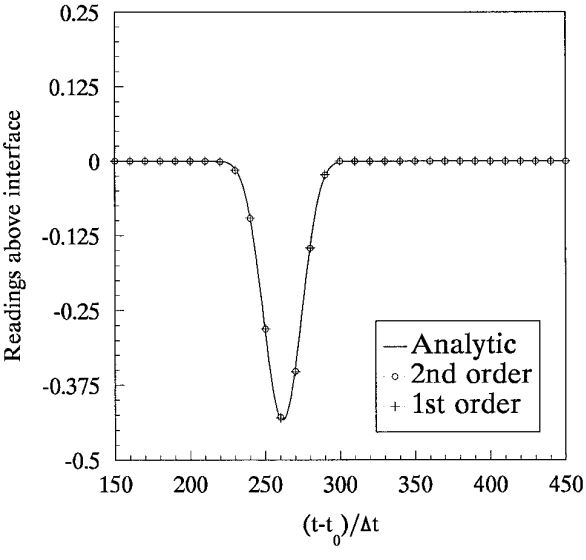

FIG. 2. Magnitude of the transmission.

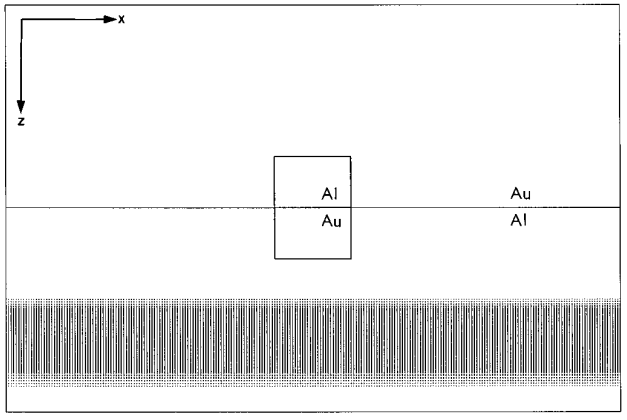

FIG. 3. Displacement field at $t = t_0$ for inverse material inclusion.

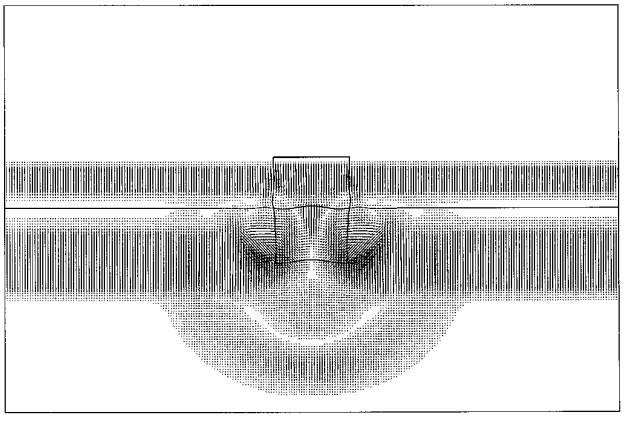

FIG. 5. Displacement field at $t = t_0 + 90h$, for inverse material inclusion.

All interfaces are assumed to be perfect bonds. Figure 3 shows the displacement field at the initial time level $t = t_0$. A compressional vertical pulse is travelling upwards before hitting the inclusions. The displacement fields at the time level $t = t_0 + 40h_t$, $t = t_0 + 90h_t$, $t = t_0 + 135h_t$, $t = t_0 + 200h_t$, and $t = t_0 + 300h_t$ are displayed in Figs. 4–8. The scattering caused by interactions at interfaces of dissimilar materials are well simulated using the generalized equations of motion (16), (24), and (29) with a second order implementation.

In the third example, we consider a uniform distribution of perfect cracks perpendicular to the interface between aluminium and gold half-spaces, see Fig. 9. Each of the cracks consists of two closed stress-free surfaces. The normal stress vector along the crack is zero and is thus continuous. The displacement vector is allowed to differ on the two sides of a crack and hence may be discontinuous across the crack. We apply to both crack faces the stress-free conditions that are derived from (29) by assuming either media 1 and 2 or media 3 and 4 being vacuum. Figures 9 and 10 show the displacement field at the initial time level $t = t_0$ and at the time level $t = t_0 + 175\ \Delta t$.

A full stability analysis for our new block media formulation is not yet available. However, the above examples have demonstrated strongly that it does provide stable numerical calculation.

5. A PARALLEL ALGORITHM

An alternative approach to the finite difference modelling is obtained after careful observations of our newly established generalized equations of motion for interfaces. It is easily seen that Eq. (29) can be regarded as a weighted average of four stress-free corner conditions with $h_1h_2\rho_1$, $h_2h_3\rho_2$, $h_3h_4\rho_3$, and $h_4h_1\rho_4$ as the weights. The four stress-free corner conditions are those obtained from (29) when three of the four media become vacuum. For example,

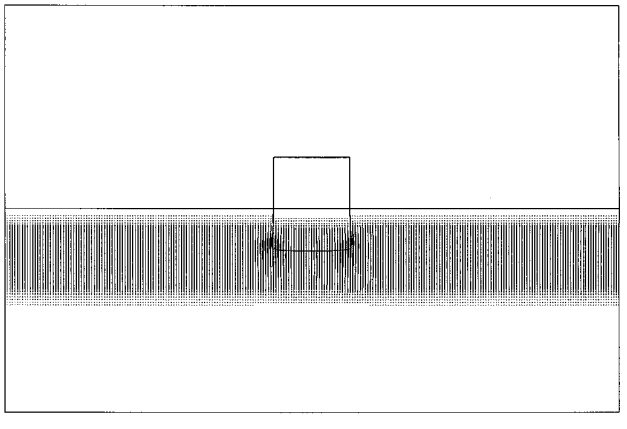

FIG. 4. Displacement field at $t = t_0 + 40h_t$ for inverse material inclusion.

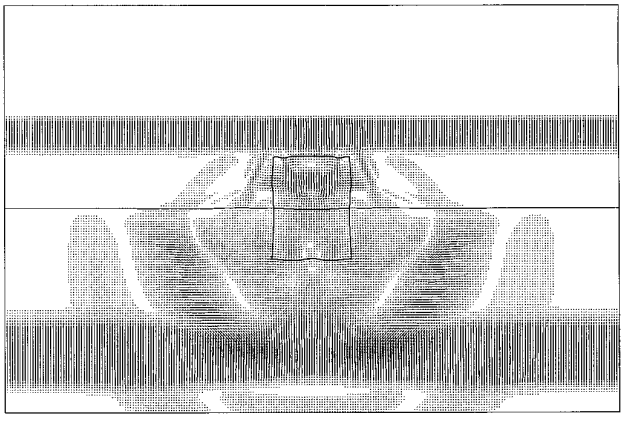

FIG. 6. Displacement field at $t = t_0 + 135h_t$ for inverse material inclusion.

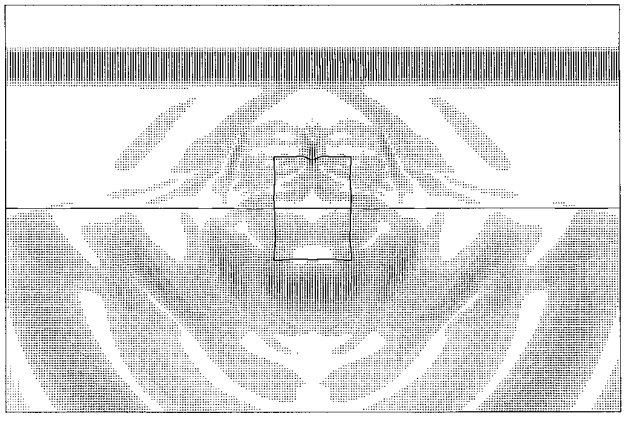

FIG. 7. Displacement field at $t = t_0 + 200h_t$ for inverse material inclusion.

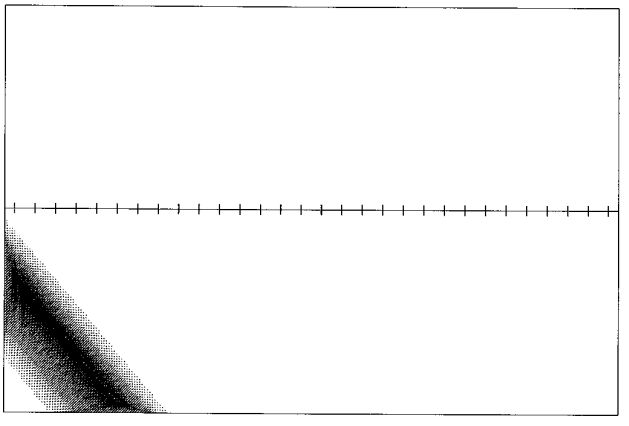

FIG. 9. Displacement field at $t = t_0$ for a distribution of vertical cracks.

$$\boldsymbol{u}_{tt} = \begin{bmatrix} \alpha_2^2 & 0 \\ 0 & \beta_2^2 \end{bmatrix} G_l^x[h_2]\boldsymbol{u}^2 + \frac{g_l}{h_2}\begin{bmatrix} 0 & \alpha_2^2 - 2\beta_2^2 \\ \beta_2^2 & 0 \end{bmatrix}\boldsymbol{u}_z^2$$
$$+ \begin{bmatrix} \beta_2^2 & 0 \\ 0 & \alpha_2^2 \end{bmatrix} G_l^z[-h_3]\boldsymbol{u}^2 - \frac{g_l}{h_3}\begin{bmatrix} 0 & \beta_2^2 \\ \alpha_2^2 - 2\beta_2^2 & 0 \end{bmatrix}\boldsymbol{u}_x^2$$
$$+ \begin{bmatrix} 0 & \alpha_2^2 + \beta_2^2 \\ \alpha_i^2 + \beta_i^2 & 0 \end{bmatrix}\boldsymbol{u}_{xz}^2 \qquad (38)$$

for the corner that is defined by $x' \geq x$ and $z' \leq z$. Similarly, Eq. (16) is the weighted average of two horizontal stress-free conditions, and (24) the weighted average of two vertical stress-free conditions. Thus forward iteration schemes like (34) can be implemented via sub-problems based on each individual homogeneous and isotropic block with horizontal and vertical stress-free surfaces and stress-free corner vertices. We give details below.

Suppose that we have computed $\boldsymbol{u}_{i,j,1}$ up to $\boldsymbol{u}_{i,j,k}$, for all i and j, and are now calculating $\boldsymbol{u}_{i,j,k+1}$. To go from level k to level $k + 1$, the original problem can be divided into many sub-problems. Each sub-problem corresponds to one homogeneous and isotropic block. Within the block, elastic wave equation (5) with appropriate parameters is imposed. On the boundary of the block, horizontal, vertical, and corner stress-free conditions based on our generalized equations of motion are also used. All sub-problems are discretized for forward iterations in time, using central differences whenever possible. Then $\boldsymbol{u}_{i,j,k+1}$ can be calculated by forward iterations using finite difference schemes for sub-problems. The values at interior nodes of sub-problems are final. For a node on a common boundary of two or more sub-problems, the final value at that node is obtained as a weighted average of the values of individual sub-problems. As an illustration, we consider the situation described in Section 3 for a interface vertex, see Fig. 11. Let us identify block 1 with sub-problem 1, block 2 with

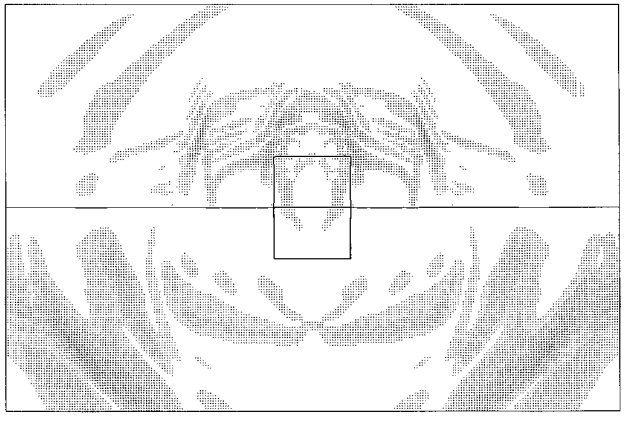

FIG. 8. Displacement field at $t = t_0 + 300h_t$ for inverse material inclusion.

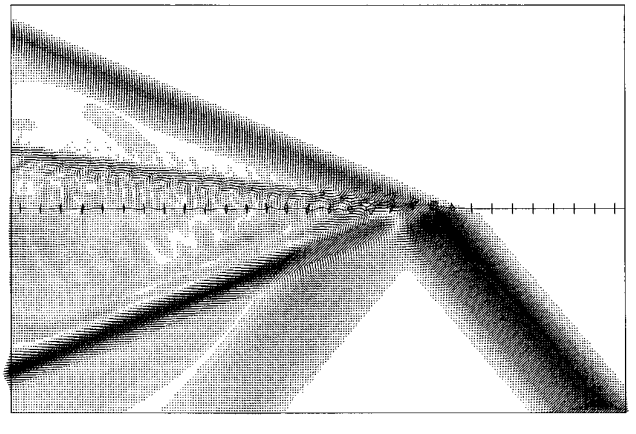

FIG. 10. Displacement field at $t = t_0 + 175h_t$ for a distribution of vertical cracks.

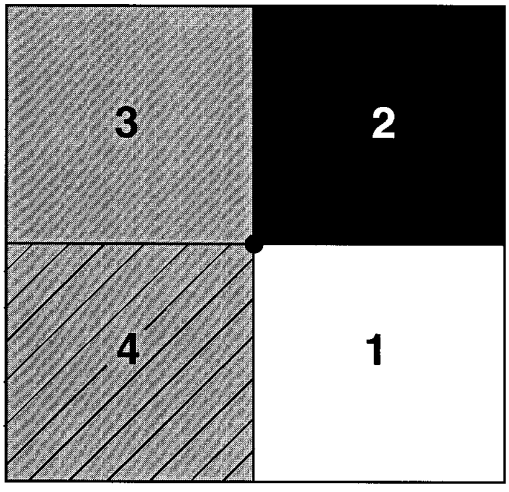

FIG. 11. Interfaces in rectangular block media.

sub-problem 2, and so on. Let us also denote $\boldsymbol{u}^{[m]}_{i,j,k+1}$ as the wave field values of sub-problem m for the new time level. Then if a point $(x_0 + ih_x, z_0 + jh_z)$ is on the horizontal interface between block 1 and block 2, the final value for the new time level at that point becomes

$$\boldsymbol{u}_{i,j,k+1} = \frac{h_{z1}\rho_1}{h_{z1}\rho_1 + h_{z2}\rho_2}\boldsymbol{u}^{[1]}_{i,j,k+1} + \frac{h_{z2}\rho_2}{h_{z1}\rho_1 + h_{z2}\rho_2}\boldsymbol{u}^{[2]}_{i,j,k+1}. \quad (39)$$

If the point is the interface vertex where all four blocks meet, the final value for the new time level will be

$$\boldsymbol{u}_{i,j,k+1} = \frac{\begin{array}{c} h_{z1}h_{x1}\rho_1\boldsymbol{u}^{[1]}_{i,j,k+1} + h_{x1}h_{z2}\rho_2\boldsymbol{u}^{[2]}_{i,j,k+1} \\ + h_{z2}h_{x2}\rho_3\boldsymbol{u}^{[3]}_{i,j,k+1} + h_{x2}h_{z1}\rho_4\boldsymbol{u}^{[4]}_{i,j,k+1} \end{array}}{h_{z1}h_{x1}\rho_1 + h_{x1}h_{z2}\rho_2 + h_{z2}h_{x2}\rho_3 + h_{x2}h_{z1}\rho_4} \quad (40)$$

This new approach has thus been readily adapted for parallel processing of the sub-problems, which improves the efficiency of the wave field computation.

6. CONCLUSIONS

We have developed a new formulation for dealing with elastic block media. By incorporating continuity conditions of stresses into the equation of motion, we are now able to represent elastic waves in media with discontinuous material parameters in a more straightforward manner. A single differential-difference equation is associated with any particular point anywhere inside the computational domain. Continuity conditions at interfaces aligned with grid lines are built in and therefore are no longer necessary to be imposed explicitly. The formulation in the form of such a differential-difference equation should be applicable to many numerical methods, although here it has been demonstrated for finite difference modelling.

Another important feature of the new block media formulation is that it effectively provides a parallel computer algorithm for computing the wave field.

One drawback of the present differential-difference formulation is that it requires a material discontinuity to be aligned with a grid line and not to lie generally between grid lines. The use of non-uniform discretization may provide a possible remedy if the grid spacings are adjusted to enforce the alignment.

The formulation is at the moment designed for a rather restrictive class of block media where all blocks after an appropriate subdivision are rectangular. Further work is needed to fully exploit the potential of its application in elastic wave propagation problems. An extension is possible for interfaces separating the media with smooth velocity and density variations. We also intend to extend our result for more general elastic block media composed of polygonal blocks so as to tackle problems involving wavy interfaces or composites, which contain essentially circular inclusions. Extension to 3D applications is also planned. We believe the results with rectangular blocks in 2D are already very encouraging.

ACKNOWLEDGMENT

This work was performed with the support of a grant awarded by the Engineering and Physical Sciences Research Council, United Kingdom.

REFERENCES

1. K. R. Kelly, R. W. Ward, S. Treitel, and R. M. Alford, *Geophysics* **41,** 2 (1976).
2. J. D. Achenbach and M. Kitahara, *J. Acoust. Soc. Am.* **80,** 1209 (1986).
3. J. D. Achenbach and Ch. Zhang, *J. Nondestr. Eval.* **9,** 71 (1990).
4. L. J. Bond, M. Punjani, and N. Saffari, *IEEE Proc.* **131,** 265 (1984).
5. N. Saffari and L. J. Bond, *J. Nondestr. Eval.* **6,** 1 (1987).
6. A. H. Harker, *Elastic Waves in Solids* (Grosvenor Press, Portsmouth, 1988).
7. L. M. Brekhovskikh, *Waves in Layered Media* (Academic Press, London, 1960).
8. B. A. Auld, *Acoustic Fields and Waves in Solids* (Wiley–Interscience, New York, 1973).
9. Z. S. Alterman and D. Loewenthal, *Geophys. J. Roy. Astron. Soc.* **20,** 101 (1970).
10. D. M. Boore, Finite difference methods for seismic wave propagation in heterogeneous materials, in *Methods of Computational Physics,* edited by B. A. Bolt (Academic Press, New York, 1972), Vol. 11.
11. J. A. G. Temple, *J. Phys. D Appl. Phys.* **21,** 859 (1988).
12. J. A. G. Temple, *Ultrasonics* **31,** 3 (1993).
13. C. A. Cunha, *Geophysics* **59,** 1840 (1993).
14. J. Zahradník and E. Priolo, *Geophys. J. Int.* **120,** 663 (1995).
15. J. Zhou and N. Saffari, *Proc. Roy. Soc. London Ser. A,* **452,** 1609 (1996).
16. A. Ilan, L. J. Bond, and M. Spvack, *Geophys. J. Roy. Astron. Soc.* **57,** 463 (1979).
17. A. Ilan, *J. Comput. Phys.* **29,** 389 (1978).
18. A. Ilan and D. Loewenthal, *Geophys. Prosp.* **24,** 431 (1976).